NASA Techanical Memorandum 113175

# Adjusting Measured Weight Loss of Aged Graphite Fabric / PMR–15 Composites

Kenneth J. Bowles
Lewis Research Center, Cleveland, Ohio

February 1998

## The NASA STI Program Office . . . in Profile

Since its founding, NASA has been dedicated to the advancement of aeronautics and space science. The NASA Scientific and Technical Information (STI) Program Office plays a key part in helping NASA maintain this important role.

The NASA STI Program Office is operated by Langley Research Center, the Lead Center for NASA's scientific and technical information. The NASA STI Program Office provides access to the NASA STI Database, the largest collection of aeronautical and space science STI in the world. The Program Office is also NASA's institutional mechanism for disseminating the results of its research and development activities. These results are published by NASA in the NASA STI Report Series, which includes the following report types:

- TECHNICAL PUBLICATION. Reports of completed research or a major significant phase of research that present the results of NASA programs and include extensive data or theoretical analysis. Includes compilations of significant scientific and technical data and information deemed to be of continuing reference value. NASA's counterpart of peer-reviewed formal professional papers but has less stringent limitations on manuscript length and extent of graphic presentations.

- TECHNICAL MEMORANDUM. Scientific and technical findings that are preliminary or of specialized interest, e.g., quick release reports, working papers, and bibliographies that contain minimal annotation. Does not contain extensive analysis.

- CONTRACTOR REPORT. Scientific and technical findings by NASA-sponsored contractors and grantees.

- CONFERENCE PUBLICATION. Collected papers from scientific and technical conferences, symposia, seminars, or other meetings sponsored or cosponsored by NASA.

- SPECIAL PUBLICATION. Scientific, technical, or historical information from NASA programs, projects, and missions, often concerned with subjects having substantial public interest.

- TECHNICAL TRANSLATION. English-language translations of foreign scientific and technical material pertinent to NASA's mission.

Specialized services that complement the STI Program Office's diverse offerings include creating custom thesauri, building customized data bases, organizing and publishing research results . . . even providing videos.

For more information about the NASA STI Program Office, see the following:

- Access the NASA STI Program Home Page at ***http://www.sti.nasa.gov***

- E-mail your question via the Internet to help@sti.nasa.gov

- Fax your question to the NASA Access Help Desk at (301) 621-0134

- Telephone the NASA Access Help Desk at (301) 621-0390

- Write to:
  NASA Access Help Desk
  NASA Center for AeroSpace Information
  800 Elkridge Landing Road
  Linthicum Heights, MD 21090-2934

NASA Techanical Memorandum 113175

# Adjusting Measured Weight Loss of Aged Graphite Fabric / PMR–15 Composites

Kenneth J. Bowles
Lewis Research Center, Cleveland, Ohio

National Aeronautics and
Space Administration

Lewis Research Center

February 1998

Trade names or manufacturers' names are used in this report for identification only. This usage does not constitute an official endorsement, either expressed or implied, by the National Aeronautics and Space Administration.

Available from

NASA Center for Aerospace Information
800 Elkridge Landing Road
Linthicum Heights, MD 21090-2934
Price Code: A03

National Technical Information Service
5287 Port Royal Road
Springfield, VA 22100
Price Code: A03

# ADJUSTING THE MEASURED WEIGHT LOSS OF AGED GRAPHITE FABRIC/PMR–15 COMPOSITES

Kenneth J. Bowles
NASA Lewis Research Center
Cleveland, Ohio 44135

## ABSTRACT

The purposes of this study were to evaluate the growth of the surface damage layer in polymer matrix composites (PMC's) fabricated with graphite fabric reinforcement and to determine the effects of the cut-surface degradation on the overall thermo-oxidative (TOS) stability of these materials. Four important conclusions were made about the TOS behavior of T650–35/PMR–15 fabric-reinforced composites: (1) Three stages of composite weight loss were seen on the plot of weight loss versus aging time; (2) the depth of the cut-edge damage is related to the composite thickness; (3) the actual weight loss realized by a mechanical test specimen that has had all the aging-induced cut-edge damage removed during the preparation process is significantly less than the weight loss measured using specimens with a high percentage of cut edges exposed to the damaging environment; and (4) an extrapolation of a section of the weight loss curve can be used to obtain a more correct estimate of the actual weight loss after extended periods of aging at elevated temperatures.

## INTRODUCTION

Comparisons of elevated-temperature, isothermal weight-loss data for different polymer matrix composite (PMC) systems are difficult to make unless the test specimens have identical geometric configurations. There is no reliable way to assess new data with published data when the specimen dimensions are different. Tests indicated that the major source of variation in the weight-loss rate during aging tests is the cut edges (Refs. 1 to 6). For the high-temperature polyimide PMR–15 matrix composites, the weight-loss rates are greater from these surfaces than from the resin-rich surfaces that are in contact with the mold surfaces or the vacuum bags during the curing of the composite material. The weight-loss rates from these unidirectional composite surfaces were actually calculated in these references. The reason the weight-loss rate is accelerated is that cracks develop parallel to the axes of the fibers that are oriented perpendicular to the cut edges of the laminates (Refs. 1 to 3). Previous work indicates that the formation and growth of cut-surface cracks occur in these fabric composites (Ref. 6). The water absorption by aged composite specimens during total immersion was measured and evaluated during that study. After long-term testing (2090 hr at 316 °C), one specimen retained enough water to fill 9 cc of new edge crack volume. Microscopic examination showed that the amount of cracking in these edges was dependent on the thickness of the composite, in addition to effects due to temperature and aging time.

The purpose of the study reported herein was to further evaluate the growth of edge cracks in composites fabricated from fabric graphite reinforcement and to determine the effects of the cut-surface degradation on the overall thermo-oxidative stability (TOS) of PMR–15 matrix composites. This information is valuable in estimating by calculation the actual weight loss of polymer matrix composites when assessing the effects of isothermal aging on the retention of mechanical properties. These areas are important because the aeronautics community is considering the use of these materials in high-temperature structures for advanced propulsion systems.

## EXPERIMENTAL

### Materials

The material used in this study was T650–35 graphite fiber/PMR–15 polyimide composite. The graphite fiber reinforcement was an 8-harness satin-weave graphite fiber fabric provided by ICI Fiberite. Laminate processing was done by autoclave techniques at the General Electric Aircraft Engine Co. in Evendale, Ohio. Curing was done at 316 °C with a free-standing postcure in an air-circulating oven at the same temperature for 16 hr. Table 1 presents the specimen designations, nominal dimensions, and nominal weights. The specimen areas and volumes are given in Table 2. The dimensions chosen provided specimens with different cut-surface to total (resin-rich and cut-surface) areas. The resin-rich surfaces are those surfaces that were adjacent to the vacuum bag containment materials during the curing process. The cut-surface areas varied from 2.7 to 89 percent of the total surface area. The numerical designations of the specimens reflect the nominal percentage of cut-edge areas. The material in this study had void contents of less than 2 percent and were free of delaminations. The fiber volume fractions ranged from 0.55 to 0.59. A typical photomicrograph of the material before aging is shown in Fig. 1.

### Test Procedures

Composite specimens were aged in air-circulating ovens with an airflow rate of 100 $cm^3$/min. The test temperatures were 204, 260, 288, 316, and 343 °C. Specimens were removed from the ovens at planned intervals, after which they were cooled to room temperature during an extended storage period in a desiccator. The specimens were removed from the desiccator only for weighing and recording. At scheduled times, selected specimens were permanently removed from the ovens for various tests.

The fiber content of the composites was measured by acid digestion as described in ASTM D–3171. The void content was calculated as the difference between the specific volume of the specimen (measured using the immersion technique as specified in ASTM D–792) and the theoretical volume (calculated from the acid digestion results). The void volume percentage was obtained by dividing the previously determined differences by the measured specific volume and multiplying by 100. The matrix and fiber densities were 1.32 and 1.78 gm/$cm^3$, respectively.

## DISCUSSION OF RESULTS

### Weight-Loss Curves

Figures 2 to 6 contain the TOS data for all the specimens that were exposed to the five elevated temperatures. These figures compare data from PMR–15 matrix composites having different geometries. It is obvious that the magnitudes of the weight losses are very sensitive to the specimen dimensional and surface characteristics. At the longer aging times, weight-loss percentages differed by as much as 10 percent. The isothermal aging of a specific specimen geometry at a specific temperature ceased when the total weight loss reached about 10 percent.

Regardless of the aging temperature or the specimen geometry, certain characteristics of the curves of aging duration and weight loss for the PMR–15 composites are evident. The first characteristic event is that all the specimens experienced an initial rapid weight loss that decreased with time at the onset of aging (Figs. 2 to 6). The time period during which this occurred varied from about 20 hr at 343 °C to greater than 2000 hr at the 204 °C aging temperature. This phase of the thermal and oxidative degradation process extends from the origin to point A in Figs. 2 to 6. Except for the T–3 and T–27 specimens, this initial weight loss is not as evident in Fig. 2 (aged at 204 °C) as it is in the data in the figures for data measured at the higher temperatures. The maximum percentage loss in weight for this specimen group appears to be around 0.5 percent during this period. The minimum weight loss was about 0.15 percent. In a separate study (Ref. 7), analysis indicated that the magnitude of the initial weight loss of the neat resin specimens was proportional to the volume of the specimen. These results are similar to those observed in Ref. 8 but are of lesser magnitude. The data in Fig. 7 support this relationship of weight loss to volume:

the data from composites aged at 343, 316, and 288 °C are straight lines; the data for the composite specimens that underwent aging at 260 °C do not follow the trend of the higher temperature curves in Fig. 8. The relationship of weight loss to volume for these data is similar to the relationship of weight loss to aging time for data shown in Figs. 2 to 6. A significant change in mechanisms apparently takes place at temperatures below 288 °C. What probably caused this change in mechanisms was that the initial release of reaction products took so long to occur that normal thermal and oxidative weight reductions increased the weight-loss values during the two lower temperature aging tests. The weight-loss amounts are 0.521, 0.310, 0.548, and 1.44 gm/cm$^3$ at 260, 288, 316, and 343 °C, respectively. Note that the maximum weight loss at 260 °C is about equal to the maximum value on the 316 °C curve. This extra weight loss probably came from thermal and oxidative reactions described above. Further crosslinking during aging, which raises the glass transition temperature $T_G$, probably produces low-molecular-weight products that diffuse from the composite during this period (Ref. 9).

The second characteristic event is the constant weight-loss rate with a positive slope shown between points A and B. Finally, after point B, the slope begins to increase and the magnitude of the slope decreases as the specimen thickness increases. This segment is considered to be dominated by the formation of new surface area that resulted from the generation of surface cracks. The weight-loss rate from the resin-rich surface is different (usually less) from that of the two cut surfaces of a unidirectional composite (see figure in Table 1). The rates of weight loss from the cut surfaces depend on the orientation of the reinforcement fibers at the surfaces. The individual weight-loss rates can be calculated mathematically by simply solving a number of simultaneous equations equal to the number of different orientations present in the different surfaces (Refs. 1, 2, 4, and 5). These studies were normally limited to specimens of the same thickness. This type of mathematical analysis did not produce consistent results with the different sizes of composite specimens used in the work described herein. The results varied when data from different combinations of specimens were used in the equations.

The specimens in this study contained only two different exposed surfaces: (1) resin-rich and (2) almost 50-50 percent fiber ends and sides. Therefore, the expectations were that weight-loss rates could be calculated in the same way for the large variety of dimensionally different specimens. This is not the case for the fabric-reinforced material we studied. The calculated surface weight-loss rates were not consistent when data from all thicknesses of thermally exposed specimens were used. The reason for this inconsistency is obvious from viewing the data in Tables 3 and 4 and in Fig. 9. The specimens shown in Fig. 9 have different thicknesses. The cross section of a 4-ply composite (T–3) is shown in Fig. 9(a). The interior and the cut-edge surface have resin-rich areas less than 0.08 mm wide. The figure also shows a constant distribution of fiber tow and neat resin pocket widths. In Fig. 9(b), the T–73 specimen is thicker (50-ply) and contains a greater amount of neat resin pockets in the interior, allowing more neat resin exposure to the cut surface and also to other interior resin pockets. It appears that the surface plies are more compressed from the curing pressure than are the plies in the interior of the composite. Therefore, the fiber content decreases slightly toward the midpoint of the thickness. This may be due in part to the lower pressure of the autoclave processing and the more tortuous paths taken by the liquified matrix to reach the outer edges. The data in Tables 3 and 4 were measured from microphotographs of mounted and polished specimens. Differential Interference Contrast (DIC) was used to enhance the difference between the surface damaged layer and the inner composite material. This process significantly reduced the gradual transition in gray tone at the “interface.” The penetration data for each pair of specimens aged at 204, 288, 316, and 343 °C for 5000, 500, 100, and 500 hr, respectively, exhibit reasonable reproducibility. Table 4 gives the measured penetration depths of the cut-edge damage for some of the aged specimens. If the data for the T–9 and T–60 specimens are compared after aging at 204 °C for 5000 hr, the thickness of the damaged layer in the T–60 specimen is about three times that in the T–9 specimen. The same is true for the T–9 and T–60 specimens aged at 288 °C for 500 hr and for the T–3 and T–12 data from specimens aged at 316 °C for 100 hr. The differences are significant. The T–3 specimens labeled full-length penetration exhibit molded-surface damage layers that exceeded the specimen thickness.

The results for specimen T–3, which was aged for a short time and contained only three percent cut surfaces, were expected to show weight-loss rates close to those of a molded, resin-rich surface. This rationale was confirmed by the damage patterns seen in Fig. 9(a). The average penetration along the cut edges (arrow B) is about the same as the penetration along the molded surfaces (arrow A). This means that the majority of weight loss occurs along the A-surfaces and the weight-loss rates along these should dominate. Conversely, specimen T–89 contains 89 percent bare cut surfaces that should exhibit total weight-loss rates similar to those of cut surfaces. The T–3, T–5, and T–12 specimens (geometrically different only in thickness) should reflect the influence of the cut surfaces on their total weight losses.

Figure 10 illustrates the differences between the areal weight-loss rates from the total specimen surfaces for the T–3, T–9, T–12, and T–89 composites. The areal weight-loss rates from the T–3 and T–9 specimens are almost identical even though T–9 has about three times more cut-surface area than T–3. It appears that the initial constant areal weight-loss rate is a good number for the resin-rich surfaces because the extra 6 percent of cut area in the T–9 specimen did not contribute significantly to an increase in the areal weight-loss rate, as illustrated in Fig. 10. The specimens in this figure are T–9 and T–50 after 5000 hr of aging at 204 °C. The average depth of the damage in the cut ends in the T–9 specimen is almost equal to the depth of damage in the molded surfaces. Thus, the total damage over the entire surface area is nominally constant. The visible penetration into the cut edges of the thicker 50-ply specimen is much deeper. This penetration and the increase in thickness may result in a higher value for the average weight loss per unit area.

Figure 11 is a plot similar to that in Fig. 10, but it compares a T–3 specimen with the thicker T–12 specimen and the T–89 specimen with the thicker T–50 specimen. The curves for the T–3 and T–12 specimens have the same slopes up to 1200 hr of aging. During the first 200 hr, there is a difference in weight loss per area that can be attributed to the volume-dependent weight loss of reaction products. Because of the narrow widths of the two specimens, they lose weight at nearly the same rate. The small increase in molded-surface area does not appear to change the total weight loss per unit area. The initial weight-loss data from these specimens seem to be typical of those from the cut surfaces.

If one compares the molded-surface changes with the cut-surface changes as the aging time elapses, the path into the interior of the specimen is more accessible from the cut ends than from the top and bottom surfaces. In Fig. 12, the specimen aged at 288 °C for 500 hr illustrates the initiation of oxidation through the cut surfaces, which consist of 50 percent cut fiber ends and 50 percent fiber lateral surfaces. The figure shows alternate tows of light gray fibers indicating the oxidative degradation of the matrix. These tows (arrow B) are those oriented perpendicular to the cut surfaces. The darker tows (arrow A) would then be those with fibers oriented parallel to the cut surfaces. These fiber/matrix tows show much less oxidation, graphic evidence of the differences in the resistance to oxygen penetration afforded by the orientation of the reinforcement fibers. The specimens cut at a 45° angle reveal the cut ends of both the warp and fill tows. Also, the thicker specimens provide more routes inward than do the thinner specimens, as is obvious in Fig. 9 which shows aged specimens built up from 4 and 50 plies. The thicker specimen exhibits a deeper damage penetration from the ends than from the resin-rich surfaces. The deepest penetration is very close to the centerline of the composite, and the shape of the damage front is somewhat parabolic (Fig. 13). Also, it is important to note that the route follows the pockets of interconnected neat resin material. These quantified differences are presented in Table 4.

## Adjusted Weight Losses

The volume data for the damaged surfaces (Table 5) were calculated by multiplying the molded and cut-surface areas by the measured layer thicknesses. The larger cut-edge thickness values were estimated by taking the average of the depths of penetration at the laminate centerline and at the molded surfaces. In Table 5, the cut-edge damaged material volume is significant even for the thinner T–3, T–5, T–9, and T–12 specimens. This suggests that, discounting the edge damage, the actual weight losses resulting from the exposure to elevated temperatures can be much smaller than the measured values of the untrimmed plates. This condition could exist in most polymer matrix composite structures considered for use in aeropropulsion structures that contain no exposed cut edges.

When the mechanical properties of aged and unaged materials are measured, the specified specimen preparation procedure is to remove and discard the edge material because it is not representative of the composite material. Therefore, the actual weight loss of the material being tested is not the measured weight loss. If the weight loss per unit volume of damaged edge material is the same as it is for the damaged molded-surface material, the theoretical weight loss for a structure without a significant amount of cut edges can be substantially less than the observed weight loss from isothermal aging tests. This is evident from Table 5. Therefore, a more realistic measure of thermal and oxidative damage should be used to correlate TOS with mechanical property changes during thermal aging tests.

Two T–5 panels (one aged for 1730 hr at 316 °C and the other at 343 °C for 670 hr) were chosen for examination to determine the approximate weight loss after the edges had been removed. Prior to the panels' being placed in the aging ovens, the dimensions were measured and the weights recorded after drying in an oven at 125 °C for 24 hr.

Nominal densities were calculated for each panel. After the panels were aged and removed from the oven and weighed, measurements showed that the 316 °C panel had lost 10.1 percent of its weight during the aging period whereas the 343 °C panel lost 11.1 percent. The aged panels were dried and weighed, and then about 3.2 mm of the edge material was trimmed. The new dimensions were measured and the resulting densities calculated. The weight losses of the trimmed panels were calculated by dividing the weight of the trimmed plate by the theoretical weight of the trimmed plate prior to aging. The unaged weight was determined by multiplying the volume of the trimmed plate by the initial calculated density. The two calculated weight losses were 4.4 and 1.5 percent, respectively (see Table 6).

The second procedure for estimating the actual weight loss experienced by the material after the damaged edges were removed from the laminates was to use the data in Table 5, which contains calculated damage volumes as measured from microphotographs. This calculation procedure was used to separate the edge damage from the resin-rich surface damage:

$$\frac{\text{Molded damage volume}}{\text{Edge damage volume} + \text{Molded damage volume}} \times \text{Total measured percentage weight loss for each laminate}$$

With this procedure, one assumes that the weight loss per unit volume of the degraded molded surface is the same as the weight loss per unit volume of the damaged cut surfaces. Calculations show that the specimen aged at 316 °C had lost 8.7 percent of its original weight through the resin-rich surfaces and that the 343 °C laminate had lost 7.5 percent. Since the adjusted weight losses of the two calculations described above do not agree, it appears that the weight losses per unit volumes of molded and cut surfaces are not identical in all cases. This is apparent from Fig. 14, which shows large void areas in the edges that were not observed in the molded surfaces.

Additional calculations of density changes were performed. The weights and dimensions of the edge strips were also measured to determine the magnitudes of changes due to the isothermal aging process. The laminates studied were aged at 204, 260, and 288 °C. A T–12 specimen aged at 288 °C for 10 080 hr and having a measured weight loss of 11.6 percent had calculated weight losses of 3.3 percent in the interior and 19.3, 26.0, 19.0, and 21.2 percent at the four edges. The widths of the edges were slightly different and were the main reason for the differences in the values. A thinner T–3 specimen aged under the same conditions and having a calculated weight loss of 13 percent was also trimmed and measured. The central material lost 8.7 percent and the outer edges lost an average of 14.6 percent. The results of all the calculations are presented in Table 6.

The third calculation procedure utilized the extrapolation of the slope between points A and B to the actual aging times (1730 and 670 hr). Thus, the increase in weight-loss rate after point B on the weight-loss plots is assumed to be caused by just the cracking that occurred. The weight loss from the resin-rich surfaces would then continue at the rate measured between points A and B. The dashed line in Fig. 15(a) indicates the data from the extrapolation for the T–5 specimens aged at 316 ∞C and the extrapolation for the T–12 specimen aged at 343 °C is shown in Fig. 15(b). The calculated percentage weight loss of the panel aged at 316 °C was 4.2 and for the panel aged at 343 °C was 2.3. All the calculated weight losses at this temperature are plotted in this figure. Two of these three calculation procedures are in reasonably good agreement, which indicates that there are major weight losses in the edges of the test panels and that the actual weight-loss rates within the central parts of the specimens remain constant from point A to the end of the aging period. The sizable weight losses in the edges confirm the results observed in the water absorption tests reported in Ref. 6. Another important result of these calculations is that they show the actual weight losses of these highly aged laminates to be less than the measured weight losses. The adjusted weight losses calculated from the data of the damaged volumes are listed in the last column of Table 5.

Measurements show a significant change in the thicknesses of the two panels. Such shrinkage behavior was previously measured and reported for neat PMR–15 specimens aged at 204, 260, and 288 °C in Ref. 7. The thickness of the panel aged at 316 °C was reduced to 93.5 percent of its original value whereas the panel aged at the higher temperature was reduced to 90.8 percent of its original thickness. It is important to understand that the total reduction in thickness is a combination of matrix shrinkage and surface resin loss by oxidation. The T–5 specimens aged at 316 and 343 °C for 1730 and 670 hr, respectively, exhibit an abundance of loose surface fibers (Fig. 16). Because of this result, one would expect surface losses to be larger at the higher aging temperatures than at the lower temperatures. This aspect of the study will receive attention at a later date.

## CONCLUSIONS

Analyses of the results of this investigation led to four conclusions concerning the thermo-oxidative behavior of T650–35/PMR–15 fabric-reinforced composites. The first is that at all the test temperatures, the weight-loss rate goes through three phases as the aging time increases: (1) the diffusion of cure reaction products from the bulk of the composite; (2) a constant rate of weight loss due to thermal and oxidative reactions that occur mainly in the matrix material; and (3) an accelerated weight-loss rate caused by thermally induced cracking in the cut surfaces of the specimens. The observed composite shrinkage through the matrix-dominated thickness is probably the reason for the crack initiation at the surfaces. The second conclusion is that the extent of edge damage is dependent on the specimen thickness. The damage penetrates farther toward the center of the specimen as the thickness increases. The penetration appears to be parabolic with the deepest penetration at the centerline of the specimen and the shortest penetration at the two points closest to the molded surfaces. The third conclusion is that the actual weight loss of a structural part without exposed cut edges is significantly less than the weight measured using specimens with a high percentage of cut edges exposed to the damaging environment. For test specimens that experienced weight losses of 10 percent or more, the molded-surface weight loss was less than 5 percent for the material examined in this study. The fourth conclusion is that extrapolated aging data from specimens with small percentages of cut-surface areas can be used to calculate weight-loss rates per unit area that are very close to the actual values for the molded surfaces. The calculation by this method is appropriate for most engineering structures. It is not possible to calculate weight-loss rates per unit surface for the cut surfaces from test data using specimens with high percentages of exposed cut surfaces because the change in oxygen penetration through crack extension increases with specimen thickness.

## REFERENCES


1. K.J. Bowles, and A. Meyers, “Specimen Geometry Effects on Graphite/PMR–15 Composites During Thermo-Oxidative Aging,” *Proceedings of 3lst International SAMPE Symposium*, 1285 (1986)
2. K.J. Bowles and G. Nowak, “Thermo-Oxidative Stability Studies of Celion 6000/PMR–15 Unidirectional Composites, PMR–15, and Celion 6000 Fiber,” *Journal of Composite Materials*, **22**, 966 (1988)
3. H. McManus, “Coupled Materials and Mechanics Analysis of Durability Tests for High Temperature Polymer Matrix Composites,” *High Temperature and Environmental Effects on Polymer Matrix Composites*, ASTMBSTPB 1302, Thomas S. Gates and Aboul-Hamed Zureick, eds. (1997)
4. F.J. Magendie, “Thermal Stability of Ceramic and Carbon Fiber Reinforced Bismaleimide Matrix Composites,” Master’s Thesis, Department of Chemical Engineering, University of Washington, Seattle, (1990)
5. J.D. Nam and J.C. Seferis, “Anisotropic Thermo-Oxidative Stability of Carbon Fiber Reinforced Polymer Composites,” *SAMPE Quarterly*, **24**, (1) 10 (1992)
6. K.J. Bowles and J.E. Kamvouris, “Penetration of Carbon Fabric Reinforced Composites by Edge Cracks During Thermal Aging,” *Journal of Advanced Materials*, **26**, (2) 2 (1995)
7. K.J. Bowles, D. Jayne, and T.A. Leonhardt, “Isothermal Aging Effects on PMR–15 Resin,” *SAMPE Quarterly*, **24**, (2) 2 (1993)
8. K.J. Bowles, “A Thermally Modified Polymer Matrix Composite Material With Structural Integrity to 371 °C,” *SAMPE Quarterly*, **24** (2) 2 (1993)
9. M.A. Meador, P.J. Cavano, and D.C. Malarik, “High Temperature Polymer Matrix Composites for Extreme Environments,” *Structural Composites: Design and Processing Technologies, Proceedings of the Sixth Annual ASM/ESD Advanced Composites Conference*, 529 (1990)

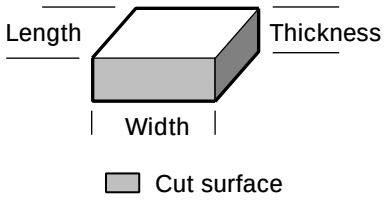


TABLE 1.—NOMINAL SPECIMEN DIMENSIONS AND WEIGHTS

| Specimen | Length, cm | Width, cm | Thickness, cm | Weight, g |
|---|---|---|---|---|
| T–3 | 8.94 | 10.80 | 0.13 | 18.5 |
| T–5 | 8.94 | 10.80 | .28 | 40.7 |
| T–9 | 9.30 | 1.56 | .13 | 2.8 |
| T–12 | 8.94 | 10.80 | .69 | 103.0 |
| T–27 | 8.90 | 10.16 | 1.70 | 243.1 |
| T–50 | 4.52 | 1.80 | 1.30 | 16.2 |
| T–73 | 6.35 | .70 | 1.74 | 12.0 |
| T–89 | 10.14 | .21 | 1.73 | 5.9 |

TABLE 2.—CALCULATED SPECIMEN AREAS AND VOLUMES

| Specimen | Volume, $cm^3$ | Surface, $cm^2$ | Molded surface, $cm^2$ | Cut-edge surface, $cm^2$ | Ratio of surface area to volume, $cm^{-1}$ |
|---|---|---|---|---|---|
| T–3 | 12.13 | 198.24 | 193.10 | 5.13 | 16.34 |
| T–5 | 27.03 | 204.15 | 193.10 | 11.05 | 7.55 |
| T–9 | 1.89 | 31.84 | 29.02 | 2.82 | 16.85 |
| T–12 | 66.62 | 211.90 | 193.10 | 18.80 | 3.18 |
| T–27 | 153.72 | 218.97 | 180.85 | 38.12 | 3.09 |
| T–50 | 10.58 | 32.70 | 16.27 | 16.43 | 3.09 |
| T–73 | 7.73 | 33.42 | 8.89 | 24.53 | 4.32 |
| T–89 | 10.50 | 40.07 | 4.26 | 35.81 | 3.82 |

TABLE 3.—MOLDED-SURFACE DAMAGE LAYER DATA

| Specimen | Temperature, °C | Time, hr | Thickness, mm | Weight loss,[a] percent |
|---|---|---|---|---|
| T–50 | 204 | 1 000 | 0.076 | 0.02 |
| T–9 | | 2 000 | .048 | .04 |
| T–50 | | 5 000 | .160 | .08 |
| T–9 | | 5 000 | .160 | .08 |
| T–12 | | 14 680 | .889 | .69 |
| T–50 | | 15 830 | .889 | .95 |
| T–50 | 260 | 1 000 | 0.064 | 0.25 |
| T–50 | | 2 000 | .122 | .44 |
| T–9 | | 3 000 | .150 | .70 |
| T–50 | | 10 000 | ----- | ----- |
| T–3 | | 12 330 | ----- | ----- |
| T–5 | | 14 348 | .381 | 7.09 |
| T–89 | | 20 000 | >6.604 | 13.69 |
| T–9 | 288 | 500 | 0.064 | 0.27 |
| T–50 | | 500 | .079 | .27 |
| T–50 | | 1 000 | .095 | .50 |
| T–50 | | 2 000 | .127 | .85 |
| T–3 | 316 | 100 | 0 | 0.44 |
| T–12 | | 100 | 0 | .44 |
| T–12 | | 500 | .097 | 1.24 |
| T–89 | | 500 | .099 | 1.24 |
| T–5 | | 1 000 | .478 | 3.60 |
| T–5 | | 1 730 | .864 | 10.00 |
| T–50 | 343 | 240 | 0.396 | 2.10 |
| T–50 | | 500 | .500 | 7.00 |
| T–3 | | 500 | .508 | 7.00 |
| T–12 | | 670 | .68 | 11.1 |

[a]Percent of weight loss of T–5 specimen at same temperature and time.

TABLE 4.—CUT-END DAMAGE LAYER DATA

| Specimen | Temperature, °C | Time, hr | Thickness, mm | Weight loss,[a] percent |
|---|---|---|---|---|
| T–50 | 204 | 1 000 | 0.419 | 0.02 |
| T–9 | | 2 000 | .203 | .04 |
| T–9 | | 5 000 | .224 | .08 |
| T–50 | | 5 000 | .813 | .08 |
| T–12 | | 14 680 | 2.159 | .69 |
| T–50 | | 15 830 | 2.235 | .95 |
| T–50 | 260 | 1 000 | 0.538 | 0.25 |
| T–50 | | 2 000 | 1.067 | .44 |
| T–9 | | 3 000 | .864 | .70 |
| T–89 | | 10 000 | Full thickness | ----- |
| T–3 | | 12 330 | Full length | ----- |
| T–5 | | 14 348 | 3.785 | 7.09 |
| T–89 | | 20 000 | Full length | 13.69 |
| T–9 | 288 | 500 | 0.135 | 0.27 |
| T–50 | | 500 | .356 | .27 |
| T–50 | | 1 000 | .719 | .50 |
| T–50 | | 2 000 | 1.303 | .85 |
| T–3 | 316 | 100 | 0.043 | 0.44 |
| T–12 | | 100 | .127 | .44 |
| T–12 | | 500 | 1.052 | 1.24 |
| T–89 | | 500 | 1.052 | 1.24 |
| T–5 | | 1 000 | 2.006 | 3.60 |
| T–5 | | 1 780 | 2.235 | 10.00 |
| T–50 | 343 | 240 | 0.711 | 2.10 |
| T–50 | | 500 | 1.397 | 7.00 |
| T–3 | | 500 | Full length | 7.00 |
| T–12 | | 670 | 3.4 | 11.1 |

[a]Percentage of weight loss of T–5 specimen at same temperature and time.

TABLE 5.—VOLUMES OF DAMAGED MATERIAL

| Specimen | Temperature, °C | Time, hr | Volume, $mm^3$ | | Surface volume, percent | Surface weight loss (adjusted), [a] percent |
|---|---|---|---|---|---|---|
| | | | Molded - surface damage layer | Cut-edge damage layer | | |
| T–50 | 204 | 1 000 | 123.6 | 688.4 | 15.2 | 0 |
| T–9 | | 2 000 | 139.3 | 57.3 | 70.8 | .03 |
| T–9 | | 5 000 | 464.3 | 63.17 | 88.0 | .07 |
| T–50 | | 5 000 | 260.3 | 1 335.8 | 16.3 | .01 |
| T–12 | | 14 680 | 17 166.6 | 4 058.9 | 80.9 | .56 |
| T–50 | | 15 830 | 1 446.4 | 3 672.1 | 28.3 | .27 |
| T–50 | 260 | 1 000 | 744.1 | 883.9 | 45.7 | 0.11 |
| T–50 | | 2 000 | 198.5 | 1 753.1 | 10.2 | .04 |
| T–9 | | 3 000 | 435.3 | 243.6 | 64.1 | .45 |
| T–89 | | 10 000 | ------- | ------- | ------ | (b) |
| T–3 | | 12 330 | ------- | ------- | ------ | (b) |
| T–5 | | 14 348 | 7 357.1 | 4 182.5 | 63.8 | 4.52 |
| T–89 | | 20 000 | --------- | --------- | ------ | (b) |
| T–9 | 288 | 500 | 0 | 38.1 | 0 | 0 |
| T–50 | | 500 | 0 | 584.9 | 0 | 0 |
| T–50 | | 1 000 | 154.6 | 1 181.3 | 11.6 | .06 |
| T–50 | | 2 000 | 206.6 | 2 140.8 | 8.8 | .07 |
| T–3 | 316 | 100 | 0 | 22.0 | 0 | 0 |
| T–12 | | 100 | 0 | 238.8 | 0 | 0 |
| T–12 | | 500 | 1 873.1 | 1 977.8 | 48.6 | .60 |
| T–89 | | 500 | --------- | --------- | ------ | (b) |
| T–5 | | 1 000 | 9 230.2 | 2 216.6 | 80.6 | 2.90 |
| T–5 | | 1 730 | 16 683.8 | 2 469.7 | 87.1 | 8.71 |
| T–50 | 343 | 240 | 644.3 | 1 168.2 | 35.5 | 0.75 |
| T–50 | | 500 | 813.5 | 2 295.3 | 26.2 | 1.83 |
| T–3 | | 500 | (b) | --------- | ------ | ----- |
| T–12 | | 670 | 13 131 | 1 880.0 | 67.2 | 7.5 |

[a]Calculated weight loss of molded surfaces only.
[b]Cannot be calculated because full thickness has been thermally damaged.

TABLE 6.—DENSITY AND ADJUSTED WEIGHT-LOSS DATA FOR UNAGED AND AGED COMPOSITES

| Specimen | Aging temperature, °C | Aging time, hr | Density, g/cm$^3$ | | Weight loss, percent | | Thickness change, mm |
|---|---|---|---|---|---|---|---|
| | | | Unaged | Aged | Middle surface | Cut-edge surface | |
| T–5 | 343 | 670 | 1.540 | 1.517 | 1.5 | 1.5 | ----- |
| T–3 | | 500 | 1.484 | 1.447 | 2.5 | 8.5 | 0.06 |
| T–5 | 316 | 1 730 | 1.523 | 1.456 | 4.4 | ----- | ----- |
| T–5 | | 500 | 1.495 | ------- | ----- | ----- | ----- |
| T–12 | | 100 | 1.558 | 1.551 | .45 | ----- | 0.14 |
| T–12 | 288 | 10 080 | 1.540 | 1.489 | 3.3 | 21 | 0.27 |
| T–3 | | 10 080 | 1.550 | 1.423 | 8.7 | 14.6 | ----- |
| T–5 | | 8 960 | 1.523 | ------- | ----- | ----- | .18 |
| T–12 | 260 | 20 000 | 1.539 | 1.564 | (a) | ----- | 0.20 |
| T–3 | | 500 | 1.502 | 1.512 | (a) | ----- | .04 |
| T–5 | 204 | 26 300 | 1.532 | 1.566 | (a) | ----- | 0.11 |
| T–3 | | 26 300 | 1.484 | 1.560 | (a) | ----- | .10 |

[a]Calculated weight gain probably due to shrinkage through the thickness.

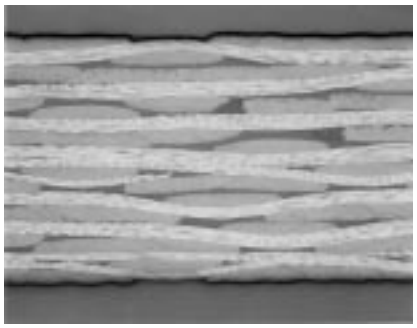

Figure 1.—Unaged T650–35/PMR–15 fabric-reinforced composite.

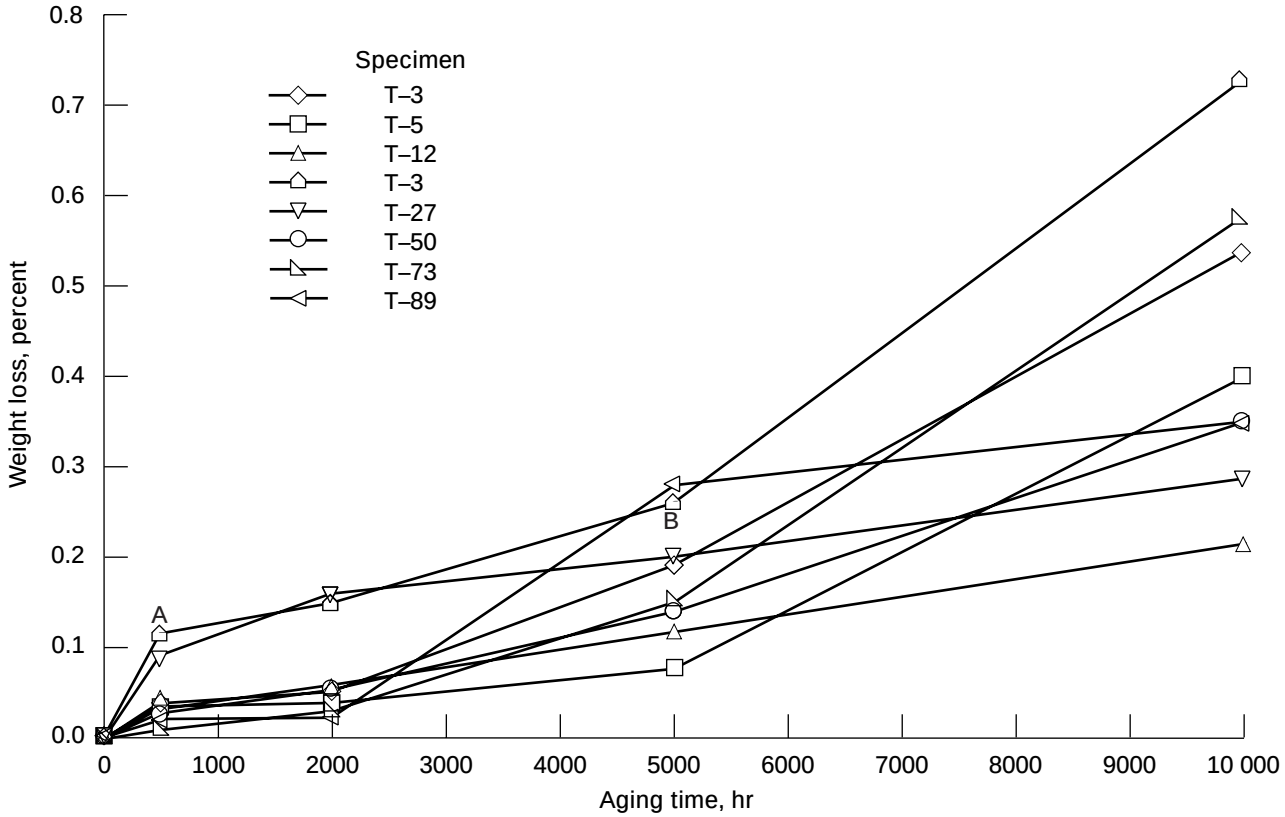


Figure 2.—Weight loss versus aging time at 204 °C.

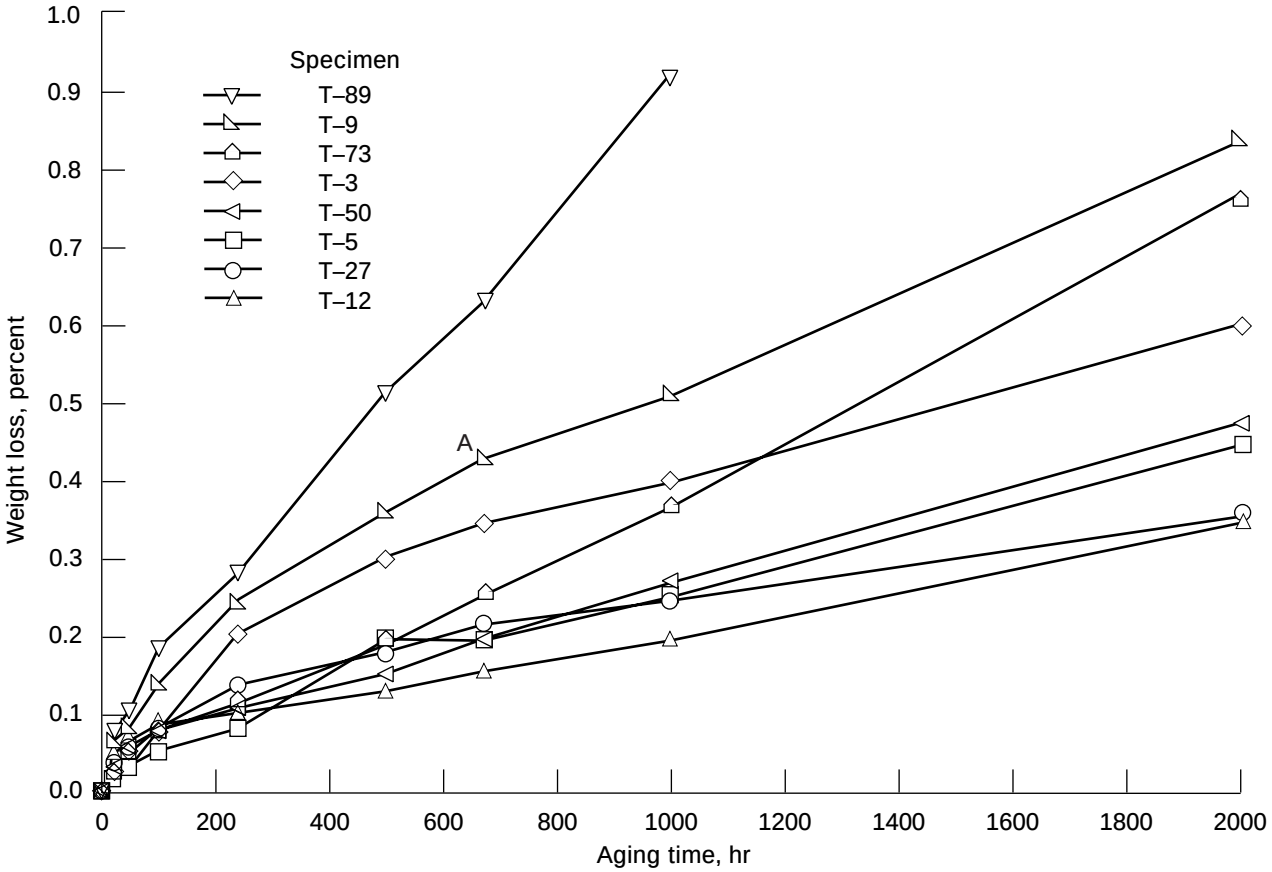


Figure 3.—Weight loss versus aging time at 260 °C.

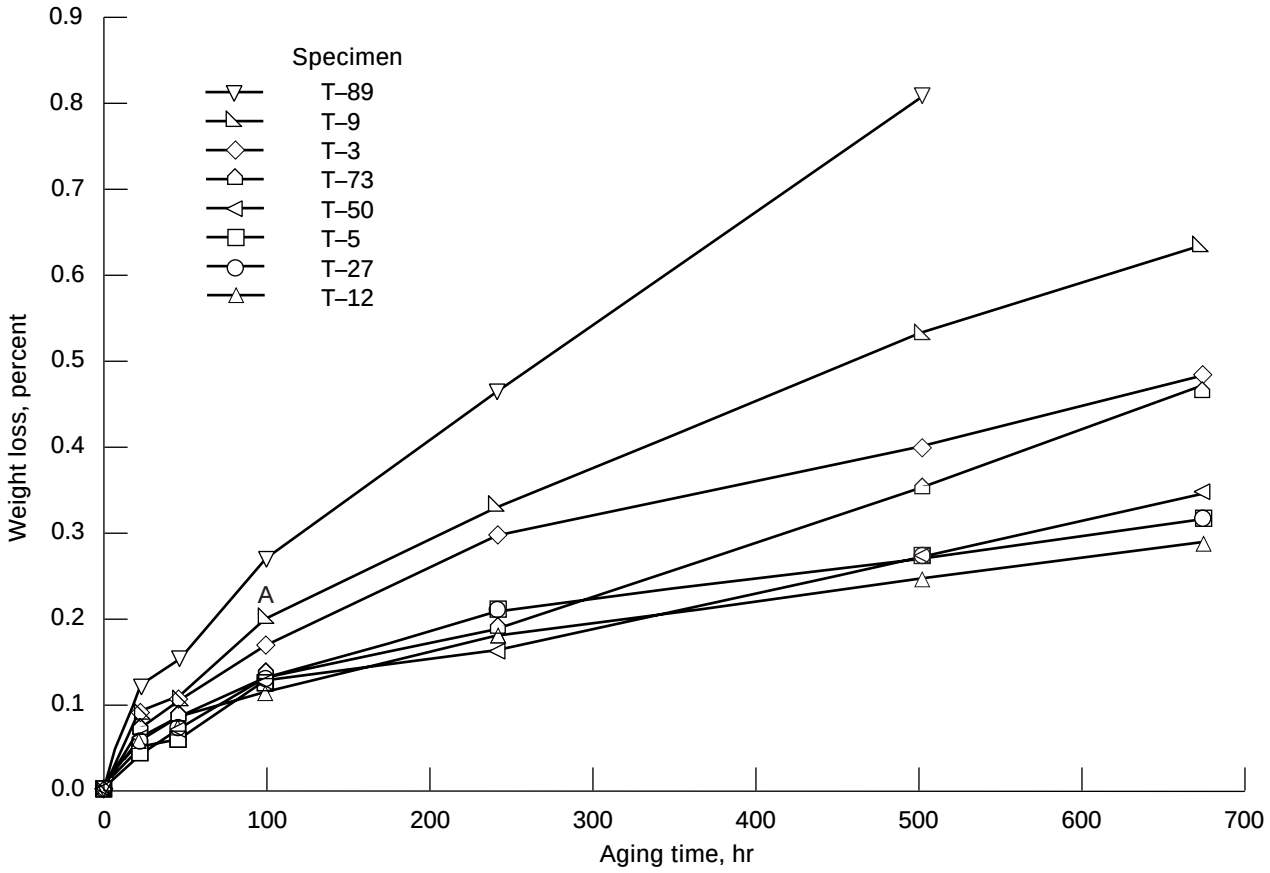


Figure 4.—Weight loss versus aging time at 288 °C.

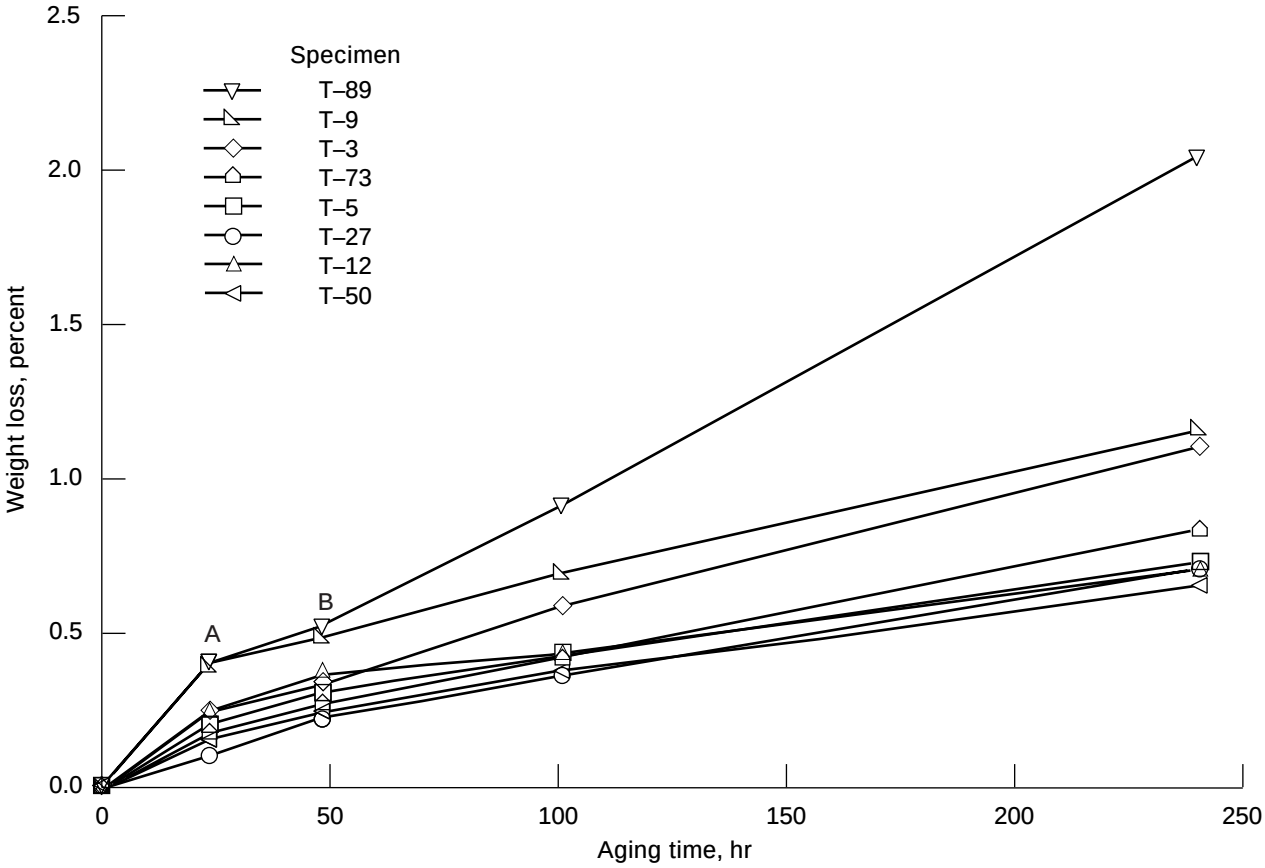


Figure 5.—Weight loss versus aging time at 316 °C.

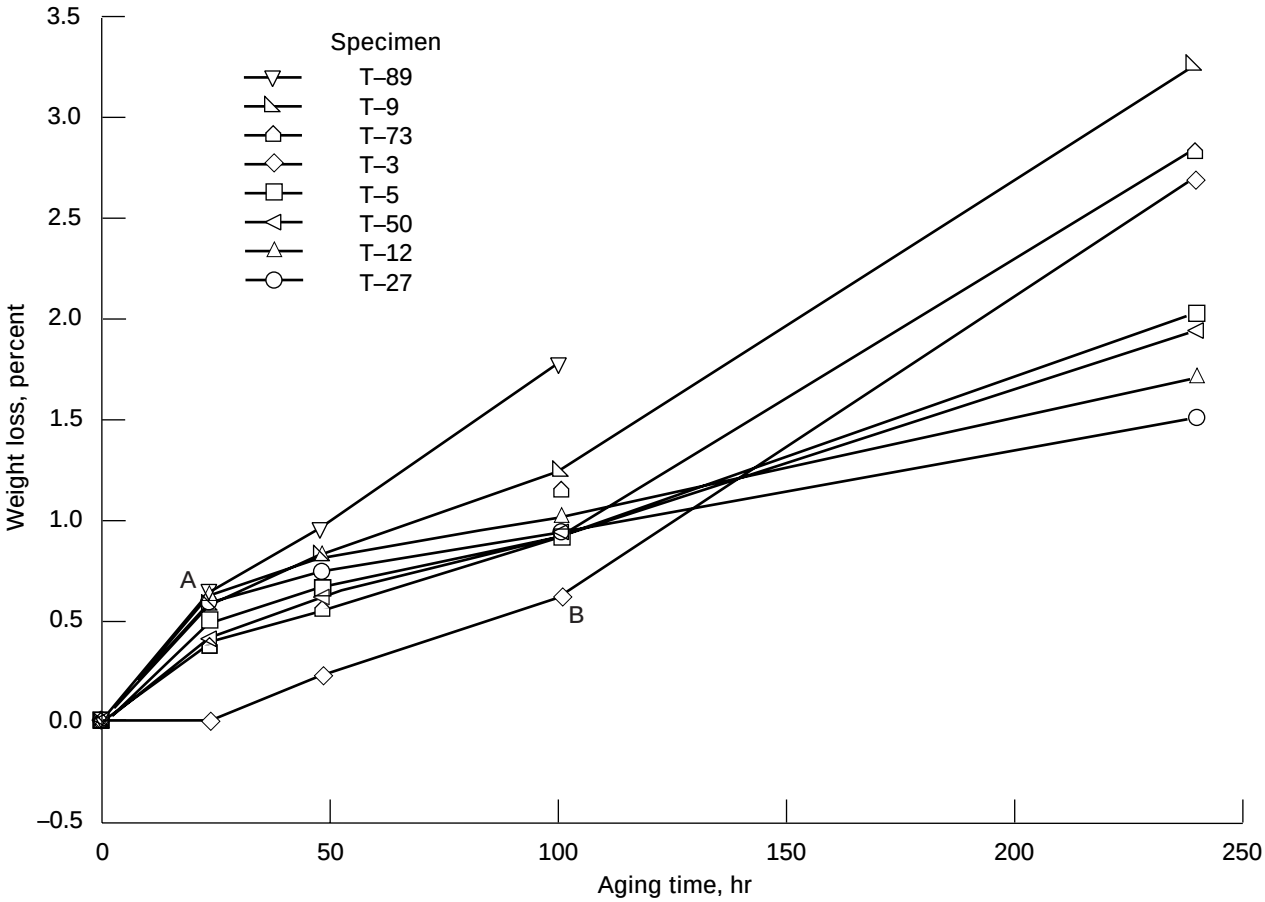


Figure 6.—Weight loss versus aging time at 343 °C.

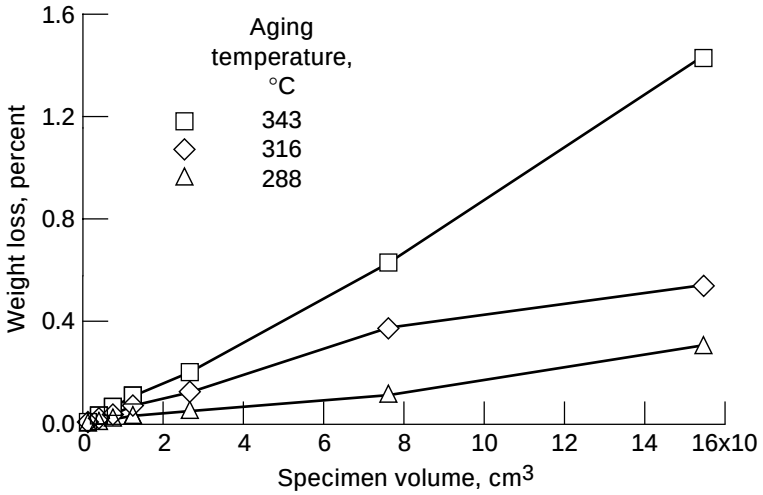


Figure 7.—Initial weight loss of different volumes of PMR–15 composites aged at various temperatures. (Volume measured at point A shown in Figs. 2 to 6.)

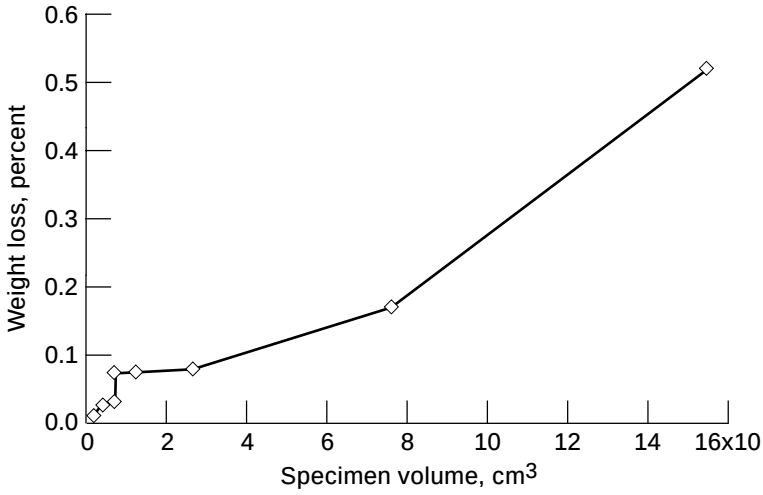


Figure 8.—Initial weight loss of different volumes of PMR–15 composites aged at 260 °C. (Volume measured at point A in Fig. 3.)

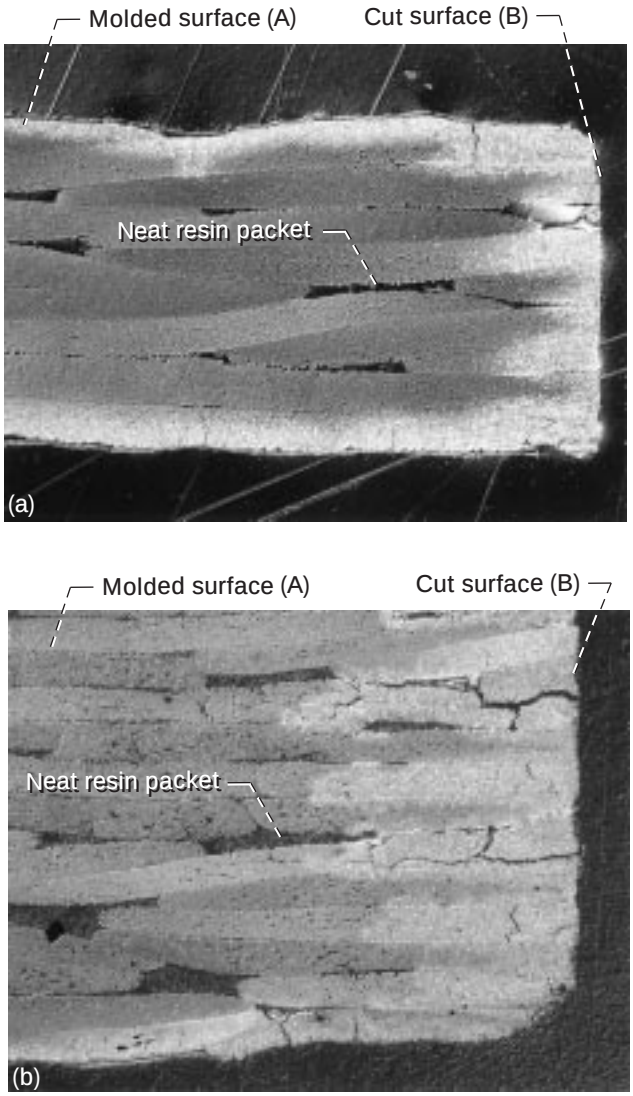


Figure 9.—Surface layer thickness for two composite specimens aged at 204 °C for 5000 hr. (a) 4-ply. (b) 50-ply.

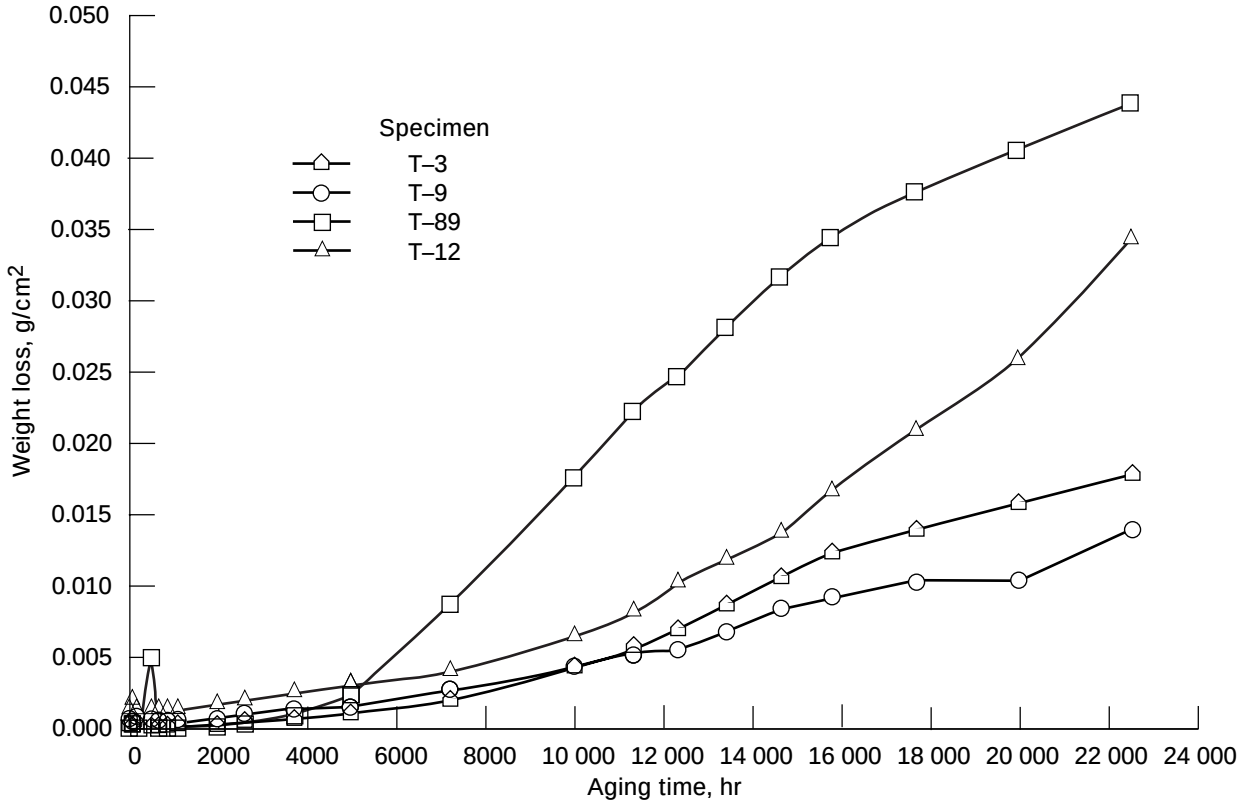


Figure 10.—Areal weight loss of T650–35/PMR–15 fabric-reinforced composites aged at 204 °C.

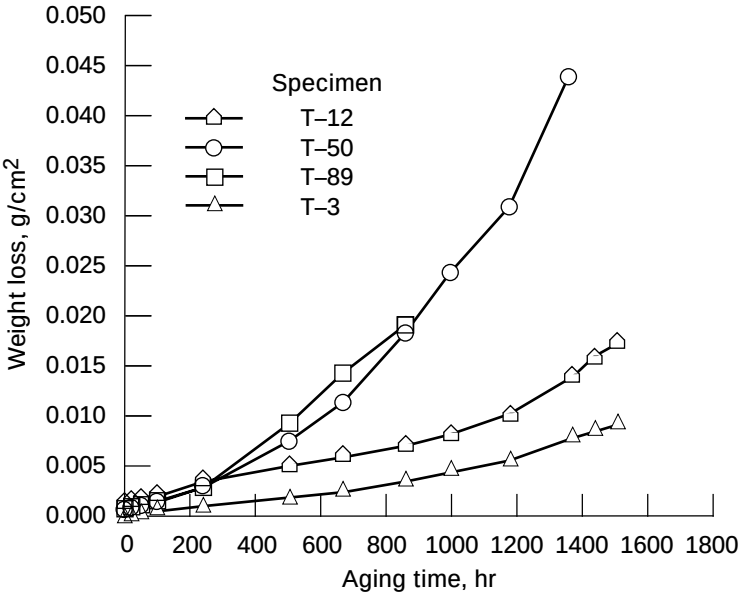


Figure 11.—Areal weight loss of T650–35/PMR–15 fabric-reinforced composites aged at 316 °C.

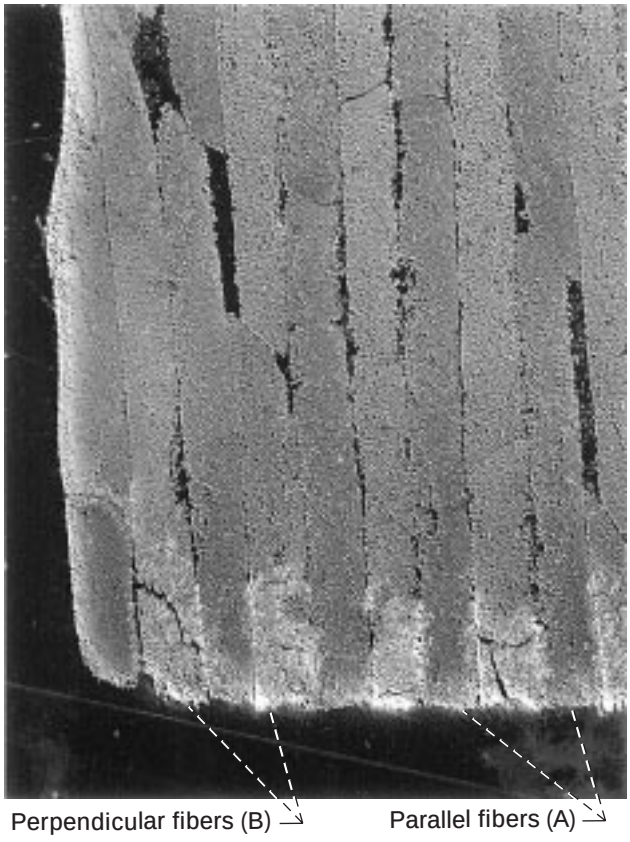


Figure 12.—Surface layer growth through reinforcement fibers of different orientations with respect to exposed surface. Specimen aged at 288 °C for 500 hr.

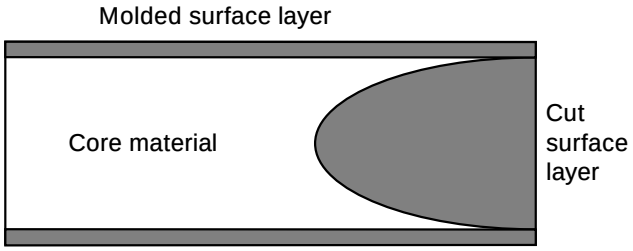


Figure 13.—Microcrack and oxidation layer growth during isothermal aging.

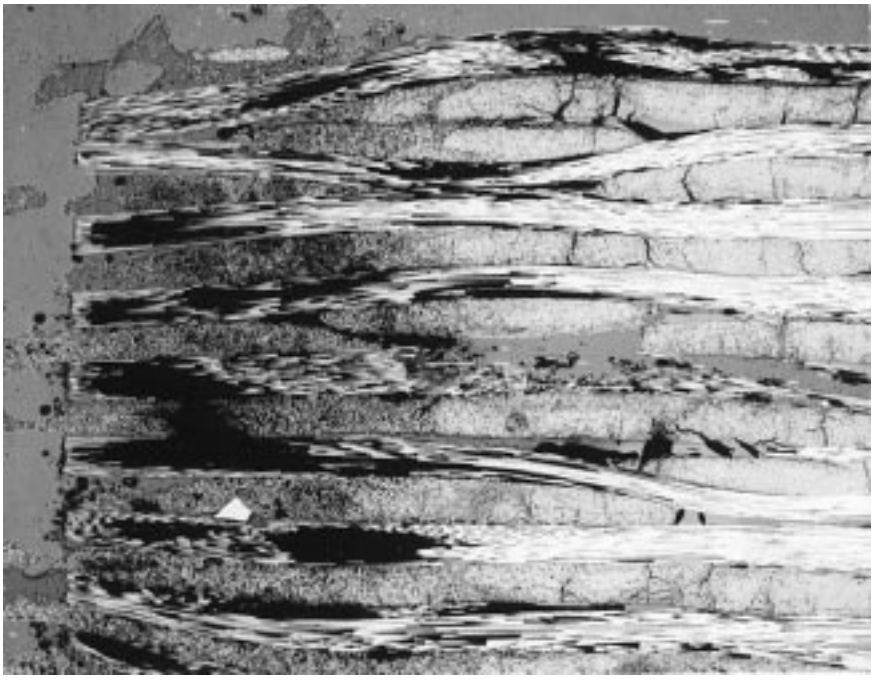

Figure 14.—Cut-edge damage of composites aged for extended period. (Note: dark areas are voids).

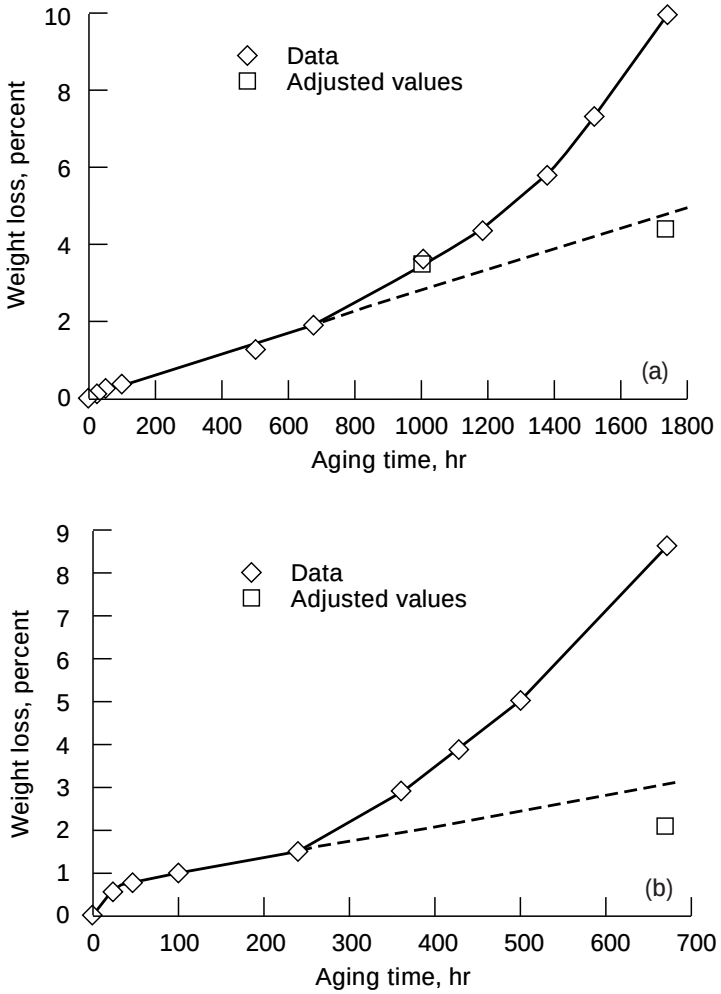


Figure 15.—Adjusted weight loss data for specimens aged at different temperatures. (a) Specimen T–5 aged at 316 °C. (b) Specimen T–12 aged at 343 °C.

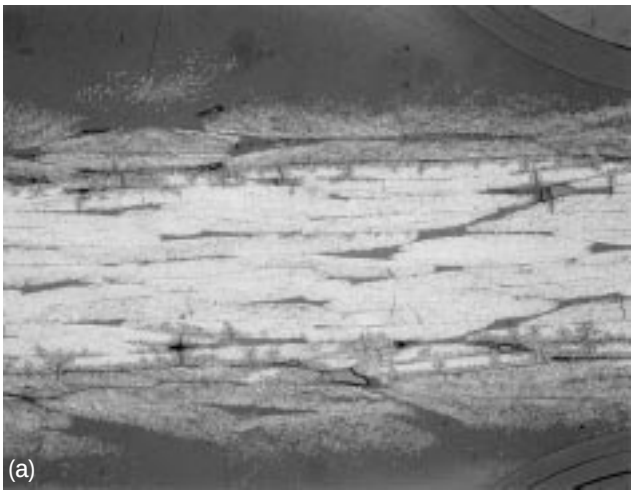


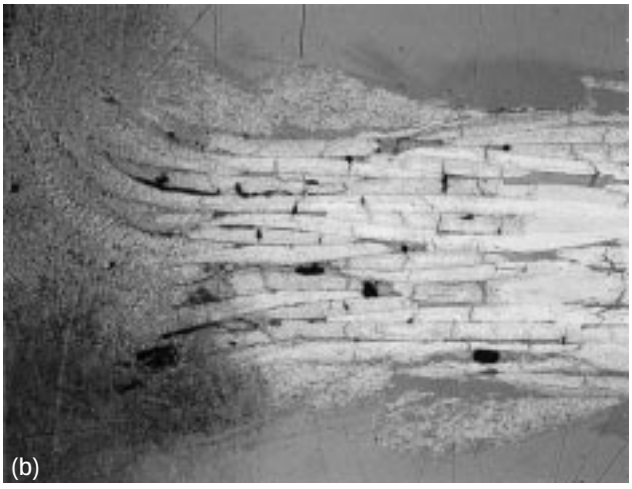


Figure 16.—Loose fibers on molded surfaces of T–5 composites. (a) Aged at 343 °C for 670 hr. (b) Aged at 316 °C for 1730 hr.

# REPORT DOCUMENTATION PAGE

*Form Approved*
*OMB No. 0704-0188*



| 1. AGENCY USE ONLY (*Leave blank*) | 2. REPORT DATE | 3. REPORT TYPE AND DATES COVERED |
|---|---|---|
| | February 1998 | Technical Memorandum |

**4. TITLE AND SUBTITLE**

Adjusting the Measured Weight Loss of Aged Graphite Fabric/PMR–15 Composites

**5. FUNDING NUMBERS**

WU–538–06–15–00

**6. AUTHOR(S)**

Kenneth J. Bowles

**7. PERFORMING ORGANIZATION NAME(S) AND ADDRESS(ES)**

National Aeronautics and Space Administration
Lewis Research Center
Cleveland, Ohio 44135–3191

**8. PERFORMING ORGANIZATION REPORT NUMBER**

E–10929

**9. SPONSORING/MONITORING AGENCY NAME(S) AND ADDRESS(ES)**

National Aeronautics and Space Administration
Washington, DC 20546–0001

**10. SPONSORING/MONITORING AGENCY REPORT NUMBER**

NASA TM–113175

**11. SUPPLEMENTARY NOTES**

Responsible person, Kenneth J. Bowles, organization code 5150, (216) 433–3197.

**12a. DISTRIBUTION/AVAILABILITY STATEMENT**

Unclassified - Unlimited
Subject Category: 24 Distribution: Nonstandard

This publication is available from the NASA Center for AeroSpace Information, (301) 621–0390.

**12b. DISTRIBUTION CODE**

**13. ABSTRACT** ***(Maximum 200 words)***

The purposes of this study were to evaluate the growth of the surface damage layer in polymer matrix composites (PMC's) fabricated with graphite fabric reinforcement and to determine the effects of the cut-surface degradation on the overall thermo-oxidative (TOS) stability of these materials. Four important conclusions were made about the TOS behavior of T650–35/PMR–15 fabric-reinforced composites: (1) Three stages of composite weight loss were seen on the plot of weight loss versus aging time; (2) the depth of the cut-edge damage is related to the composite thickness; (3) the actual weight loss realized by a mechanical test specimen that has had all the aging-induced cut-edge damage removed during the preparation process is significantly less than the weight loss measured using specimens with a high percentage of cut edges exposed to the damaging environment; and (4) an extrapolation of a section of the weight loss curve can be used to obtain a more correct estimate of the actual weight loss after extended periods of aging at elevated temperatures.

| 14. SUBJECT TERMS | 15. NUMBER OF PAGES |
|---|---|
| Polymer matrix composites; Graphite fiber fabric; Aging tests; Thermo-oxidative stability; Weight loss; Modeling | 29 |
| | 16. PRICE CODE: A03 |

| 17. SECURITY CLASSIFICATION OF REPORT | 18. SECURITY CLASSIFICATION OF THIS PAGE | 19. SECURITY CLASSIFICATION OF ABSTRACT | 20. LIMITATION OF ABSTRACT |
|---|---|---|---|
| Unclassified | Unclassified | Unclassified | |